

## **Supporting Information for:**

### **Theoretical study on the mechanisms, kinetics and risk assessment of OH radical and Cl atom initiated transformation of HCFC-235fa in the atmosphere**

Tai-Xing Chi,<sup>a</sup> Xin-Xin Li,<sup>a</sup> Shuang Ni,<sup>a</sup> Feng-Yang Bai,<sup>\*a,b</sup> Xiu-Mei Pan,<sup>\*c</sup> and Zhen Zhao<sup>a,d</sup>

<sup>a</sup>Institute of Catalysis for Energy and Environment, College of Chemistry and Chemical Engineering, Shenyang Normal University, Shenyang 110034, People's Republic of China

<sup>b</sup>Key Laboratory of Cluster Science, Ministry of Education of China, School of Chemistry and Chemical Engineering, Beijing Institute of Technology, Beijing 100081, People's Republic of China

<sup>c</sup>Institute of Functional Material Chemistry, National & Local United Engineering Lab for Power Battery, Faculty of Chemistry, Northeast Normal University, Changchun 130024, People's Republic of China

<sup>d</sup>State Key Laboratory of Heavy Oil Processing, China University of Petroleum, Chang Ping, Beijing 102249, People's Republic of China.

---

\* First corresponding author: [baify492@nenu.edu.cn](mailto:baify492@nenu.edu.cn) (Feng-Yang Bai)

\* Joint corresponding author: [panxm460@nenu.edu.cn](mailto:panxm460@nenu.edu.cn) (Xiu-Mei Pan)

**Supporting Information list:**

**S1.1 Explanation of the calculation of the effective atmospheric lifetime ( $\tau_{\text{eff}}$ ).**

**S1.2 Acidification potential.**

**S1.3 Detailed description of the toxicity assessment software ECOSAR.**

**Figure S1a.** Geometries parameters of the reactants, products, transition states, and complexes for the hydrogen abstraction channels of  $\text{CF}_3\text{CH}_2\text{CClF}_2$  by OH radical and Cl atom at the B3LYP/6-311G(2d,d,p) level. Bond lengths are in angstroms.

**Figure S1b.** Optimized geometries parameters (in Å) of all transition states (TSs) at the level of M06-2X/6-311+G(d,p). Bond lengths are in angstroms.

**Figure S1c.** Geometries parameters of the reactants, products, transition states, and complexes for the hydrogen abstraction channels of  $\text{CF}_3\text{CH}_2\text{CClF}_2$  (R1a) by OH radical and Cl atom at the M062-X/6-311+G(d,p) level. Bond lengths are in angstroms.

**Figure S2.** Calculated OH-controlled, Cl-controlled and  $\tau_{\text{eff}}$  of  $\text{CF}_3\text{CH}_2\text{CClF}_2$  determined by  $[\text{OH}]$  of  $9.0 \times 10^5$  molecules  $\text{cm}^{-3}$  and  $[\text{Cl}]$  of  $10^6$  atoms  $\text{cm}^{-3}$ . The rate coefficients were calculated at the CCSD(T)/aug-cc-pVTZ//M06-2X/6-311+G(d,p) level.

**Figure S3.** Calculated HCFC-235fa loss against altitude in the troposphere (different temperatures). ( $L^{\text{HCFC-235fa}} = k^{\text{HCFC-235fa}} \times [\text{OH}]$ ) (Where  $[\text{OH}]$  is the concentration of OH radical ( $[\text{OH}] = 10^6$  molecule  $\text{cm}^{-3}$ ) and  $k^{\text{HCFC-235fa}}$  denotes the rate constant of HCFC-235fa reacting with OH radical at 216.69–298.15 K.  $L^{\text{HCFC-235fa}}$  shows the ability that HCFC-235fa can react with OH radical to form  $\text{CF}_3\text{C-CClF}_2$  radical.) The rate coefficients were calculated at the CCSD(T)/aug-cc-pVTZ//M06-2X/6-311+G(d,p) level.

**Table S1a.** Calculated frequencies ( $\text{cm}^{-1}$ ) of the reactants, products, transition states and complexes at the level of M06-2X/6-311+G (d,p). (The value of the scaling factor is 0.970)

**Table S1b.** Relative Energies (in kcal/mol) of the reactions of  $\text{CF}_3\text{CH}_2\text{CClF}_2$  (R1a) + OH/Cl calculated at the CBS-QB3, CCSD(T)/6-311++G(d,p)//M06-2X/6-311+G(d,p) and CCSD(T)/aug-cc-pVTZ//M06-2X/6-311+G(d,p) levels of theory.

**Table S1c.** Relative Energies (in kcal/mol) of the reactions of  $\text{CF}_3\text{CH}_2\text{CClF}_2$  (R1a) + OH/Cl calculated at M062-X/6-311+G(d,p) level of theory.

**Table S1d.** The change of Gibbs free energy and Enthalpies (in kcal/mol) of the reactions of  $\text{CF}_3\text{CH}_2\text{CClF}_2$  (R1a) + OH/Cl calculated at the CBS-QB3, CCSD(T)/6-311++G(d,p)//

M06-2X/6-311+G(d,p) and CCSD(T)/aug-cc-pVTZ//M06-2X/6-311+G(d,p) levels of theory.

**Table S2a.** Multistructural torsional anharmonicity factors of  $\text{CF}_3\text{CH}_2\text{CClF}_2$ , TS1a and  $\text{CF}_3\text{CH}_2\text{CClF}_2 + \text{OH}$ , as well as the rate coefficients ( $\text{cm}^3 \text{molecule}^{-1} \text{s}^{-1}$ ) of TST, CVT, CVT/TST, SCT, CVT/SCT and MS-CVT/SCT for the reaction of  $\text{CF}_3\text{CH}_2\text{CClF}_2 + \text{OH}$  at 200–1000 K. (<sup>a</sup>CCSD(T)/6-311++G(d,p)//M06-2X/6-311+G(d,p) level. <sup>b</sup>CCSD(T)/aug-cc-pVTZ //M06-2X/6-311+G(d,p) level.)

**Table S2b.** Multistructural torsional anharmonicity factors of  $\text{CF}_3\text{CH}_2\text{CClF}_2$ , TS2a and  $\text{CF}_3\text{CH}_2\text{CClF}_2 + \text{Cl}$ , as well as the rate coefficients ( $\text{cm}^3 \text{molecule}^{-1} \text{s}^{-1}$ ) of TST, CVT, CVT/TST, SCT, CVT/SCT and MS-CVT/SCT for the reaction of  $\text{CF}_3\text{CH}_2\text{CClF}_2 + \text{Cl}$  at 200–1000 K. (<sup>a</sup>CCSD(T)/6-311++G(d,p)//M06-2X/6-311+G(d,p) level. <sup>b</sup>CCSD(T)/aug-cc-pVTZ//M06-2X/6-311+G(d,p) level.)

**Table S3a.** Zero-point energy (ZPE), vibrational ground-state adiabatic potential energy ( $V_a^G$ ) and classical potential energy ( $V_{MEP}$ ) for the reaction of  $\text{CF}_3\text{CH}_2\text{CClF}_2 + \text{OH}$  as functions of the intrinsic coordinate  $s$  (amu)<sup>1/2</sup>bohr at M06-2X/6-311+G(d,p) level.

**Table S3b.** Zero-point energy (ZPE), vibrational ground-state adiabatic potential energy ( $V_a^G$ ) and classical potential energy ( $V_{MEP}$ ) for the reaction of  $\text{CF}_3\text{CH}_2\text{CClF}_2 + \text{Cl}$  as functions of the intrinsic coordinate  $s$  (amu)<sup>1/2</sup>bohr at M06-2X/6-311+G(d,p) level.

**Table S4a.** Calculated atmospheric lifetime ( $\tau$ ) values for  $\text{CF}_3\text{CH}_2\text{CClF}_2$  determined by OH radical at variable temperatures (T) and altitudes (H) in the earth atmosphere according to the rate coefficients ( $k_{OH}^{MS - CVT/SCT}$ ). The rate coefficients were calculated at the CCSD(T)/aug-cc-pVTZ//M06-2X/6-311+G(d,p) level.

**Table S4b.** Calculated atmospheric lifetime ( $\tau$ ) values for  $\text{CF}_3\text{CH}_2\text{CClF}_2$  determined by Cl atom at different temperatures (T) and altitudes (H) in the earth atmosphere according to the rate coefficients ( $k_{Cl}^{MS - CVT/SCT}$ ). The rate coefficients were calculated at the CCSD(T)/aug-cc-pVTZ//M06-2X/6-311+G(d,p) level.

**Table S4c.** Calculated OH-controlled, Cl-controlled and effective atmospheric lifetime (unit: years) of  $\text{CF}_3\text{CH}_2\text{CClF}_2$  at minimum [OH] of  $9.0 \times 10^5$  molecules  $\text{cm}^{-3}$  and at maximum [Cl] of  $10^6$  atoms  $\text{cm}^{-3}$  at variable temperatures (T) and altitudes (H).

**Table S5.** Calculated atmospheric lifetimes at 216.69-298.15 K and global warming potentials (GWPs) of  $\text{CF}_3\text{CH}_2\text{CClF}_2$  for the time horizons of 20, 100, and 500 years at the level of CCSD(T)/aug-cc-pVTZ//M06-2X/6-311+G(d,p).

**Table S6.** ECOSAR toxicity values of  $\text{CF}_3\text{CH}_2\text{CClF}_2$  (R1a) and its degradation products to aquatic organisms (unit:  $\text{mg L}^{-1}$ ).

**Table S7.** The acute and chronic toxic class (unit:  $\text{mg L}^{-1}$ ).

### **S1.1 Explanation of the calculation of the effective atmospheric lifetime ( $\tau_{\text{eff}}$ ).**

The reason why the contribution of other processes such as photolysis, reaction with nitrate radical or ozone molecule, and deposition processes been ignored in the calculation of the effective lifetime:

In order to precisely assess the environmental impact of  $\text{CF}_3\text{CH}_2\text{CClF}_2$  in the atmosphere, the effective lifetime ( $\tau_{\text{eff}}$ ) was calculated while considering the combined constraints of OH radical and Cl atom. While no photolysis lifetime for  $\text{CF}_3\text{CH}_2\text{CClF}_2$  has been reported to date, Burkholder et al.<sup>[1]</sup> have mentioned that photolysis of most HCFCs occurs in the short-wavelength UV region (in the stratosphere) but is generally a minor loss process in comparison to free radical reaction losses. The reaction of nitrate radical with hydrocarbons was reported to be an inefficient process by Burkholder et al.,<sup>[1]</sup> and the reactivity of nitrate radical with HCFCs and HFCs is expected to be similar to or even lower than that of hydrocarbons. In addition, the loss of gas resulting from the reaction with nitrate radical is negligible compared to the loss resulting from the reaction with OH radical. Moreover, the reaction of ozone molecules with saturated halogenated species in the atmosphere is unimportant.<sup>[2]</sup> Due to the lack of information on this HCFC's wet and dry deposition, this factor is considered insignificant.

### **S1.2 Acidification potential.**

Acid rain is a significant environmental problem due to its harmful effects. The compounds containing F, Cl, N, and S atoms react with atmospheric substances to form acidic molecules. Manonmani et al. have calculated the acidification potential of fluorinated compounds.<sup>[3-4]</sup> Since HCFC-235fa contains five F atoms and one Cl atom, it is necessary to calculate the acidification

potential of HCFC-235fa. The acidification potential calculation provides information on the contribution of HCFC-235fa to acid rain compared to SO<sub>2</sub> (reference compound), using the expression:

$$AP = \frac{M_{SO_2}}{M_{CF_3CH_2CClF_2}} \left( \frac{1}{2} (n_{Cl} + n_F + n_N + n_S) \right)$$

(5)

where  $M$  is the molecular weight of SO<sub>2</sub> and HCFC-235fa, respectively, and  $n_F$ ,  $n_{Cl}$ ,  $n_N$ , and  $n_S$  represent the number of fluorine, chlorine, nitrogen, and sulfur atoms in compound HCFC-235fa. The acidification potential of HCFC-235fa was calculated to be 1.141. Thus, it can be speculated that it contributes to acid rain formation because its acidification potential is higher than that of sulfur dioxide (AP = 1 (high)).<sup>[5]</sup>

### S1.3 Detailed description of the toxicity assessment software ECOSAR.

The model uses measured data to predict the toxicity of chemicals lacking data by using structure activity relationships (SARs) and quantitative structure activity relationships (QSARs) that estimate a chemical's acute toxicity and chronic toxicity when data are available. ECOSAR contains a library of chemical class-based QSARs for predicting aquatic toxicity. It is necessary to point out that LC50 describes the amount of chemical inhaled by test animals that causes death in 50% of the test animals used during a toxicity test study. In contrast, the EC50 describes the chemicals inhaled by test animals that cause a specific effect (e.g., growth inhibition) in 50% of the test animals in a toxicity test study. Additionally, the chronic toxicity of the three aquatic organisms is expressed through the calculation of chronic toxicity values (ChV). These values serve as a foundational metric for assessing the long-term deleterious effects of the tested substances on aquatic life. The ranges

of biologically harmful values are shown in Table S7.

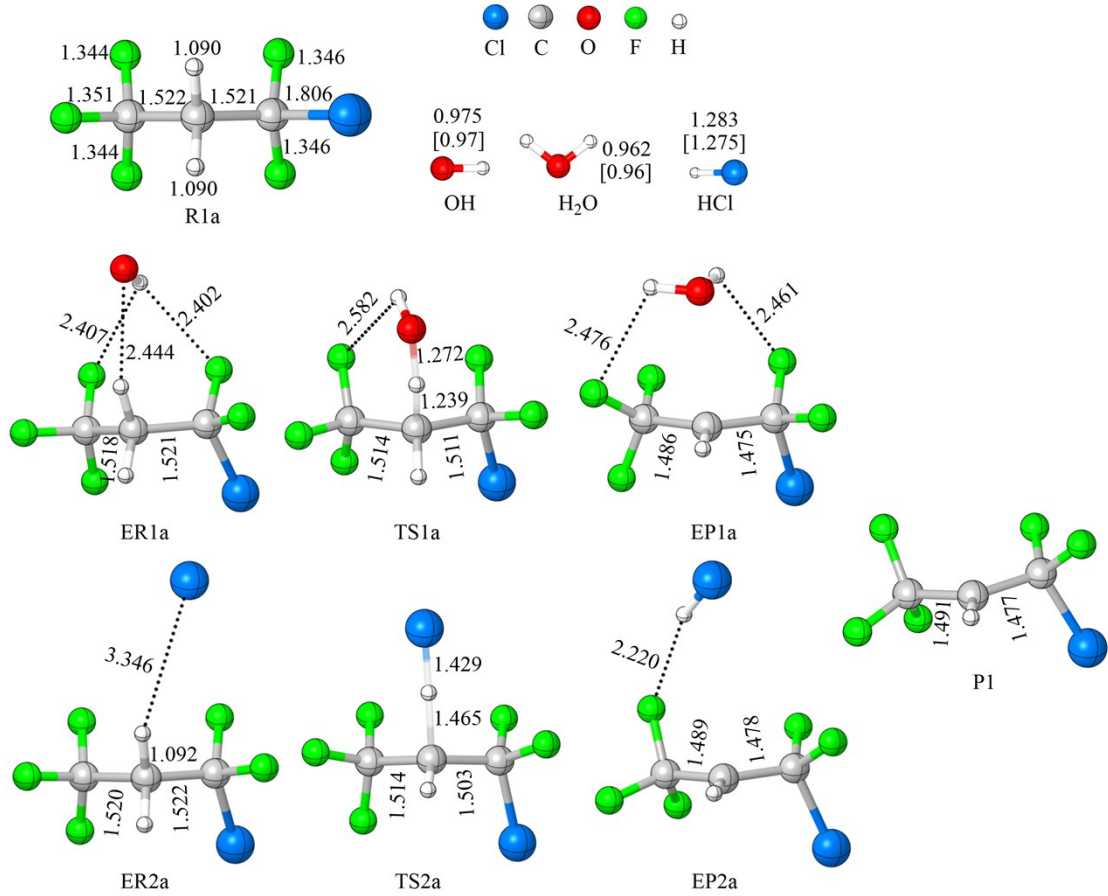


**Figure S1a.** Geometries parameters of the reactants, products, transition states, and complexes for the hydrogen abstraction channels of  $\text{CF}_3\text{CH}_2\text{CClF}_2$  by OH radical and Cl atom at the B3LYP/6-311G(2d,d,p) level. Bond lengths are in angstroms.

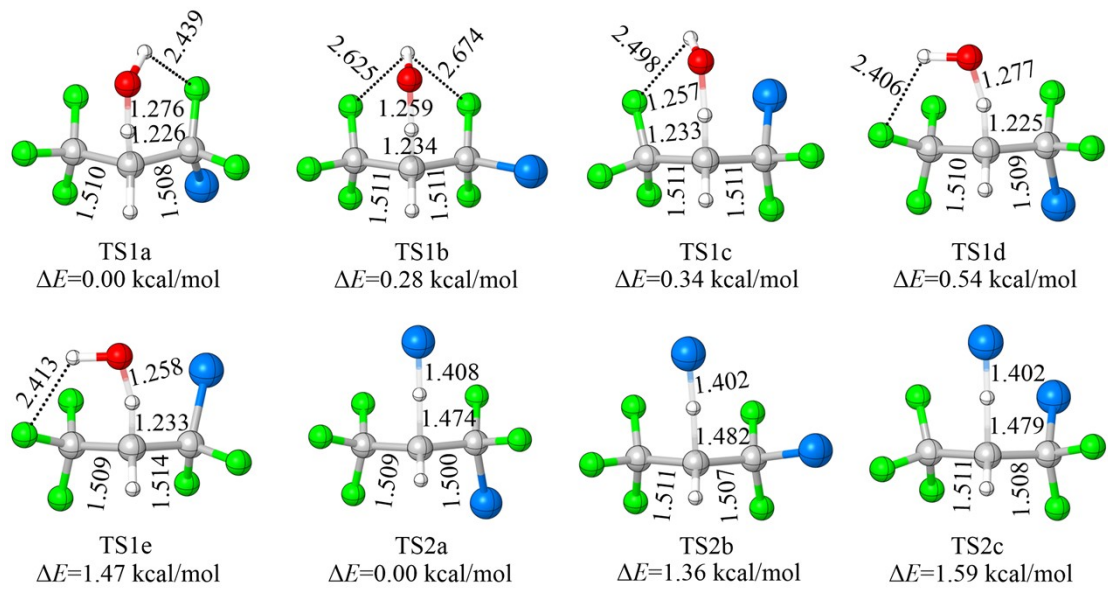


**Figure S1b.** Optimized geometries parameters (in Å) of all transition states (TSs) at the level of M06-2X/6-311+G(d,p). Bond lengths are in angstroms.

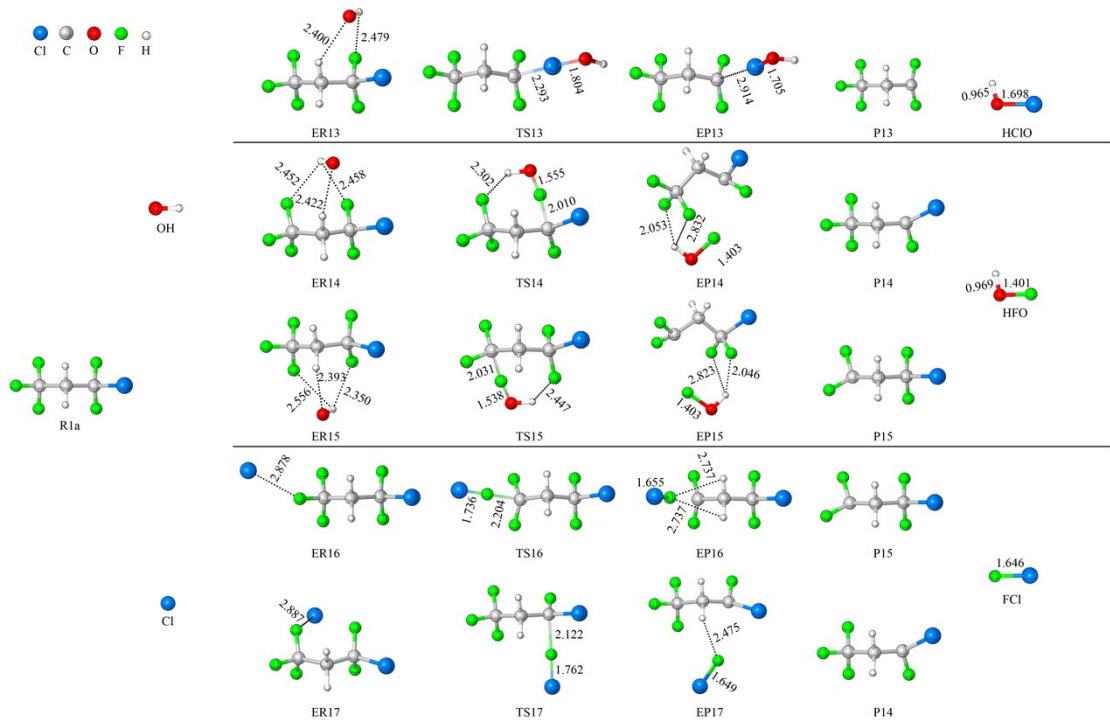


**Figure S1c.** Geometries parameters of the reactants, products, transition states, and complexes for the hydrogen abstraction channels of  $\text{CF}_3\text{CH}_2\text{CClF}_2$  (R1a) by OH radical and Cl atom at the M062-X/6-311+G(d,p) level. Bond lengths are in angstroms.

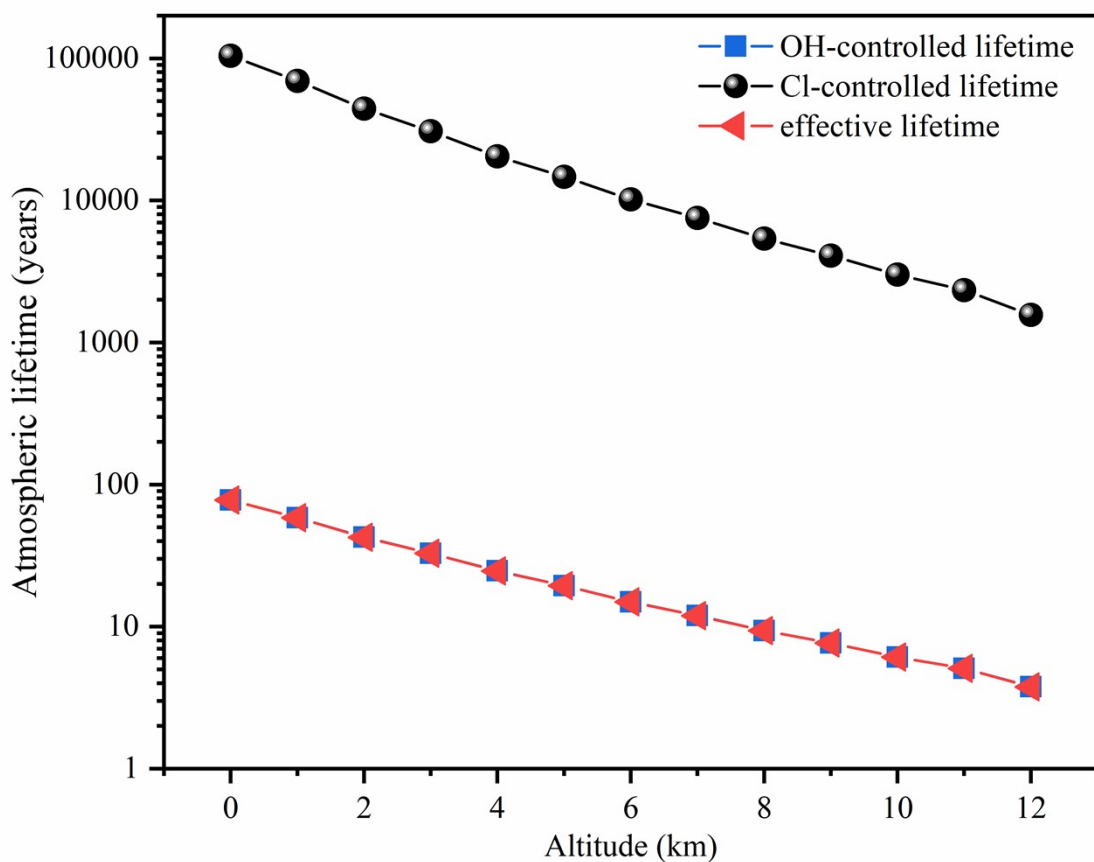


**Figure S2.** Calculated OH-controlled, Cl-controlled and  $\tau_{\text{eff}}$  of  $\text{CF}_3\text{CH}_2\text{CClF}_2$  determined by  $[\text{OH}]$  of  $9.0 \times 10^5$  molecules  $\text{cm}^{-3}$  and  $[\text{Cl}]$  of  $10^6$  atoms  $\text{cm}^{-3}$ . The rate coefficients were calculated at the CCSD(T)/aug-cc-pVTZ//M06-2X/6-311+G(d,p) level.

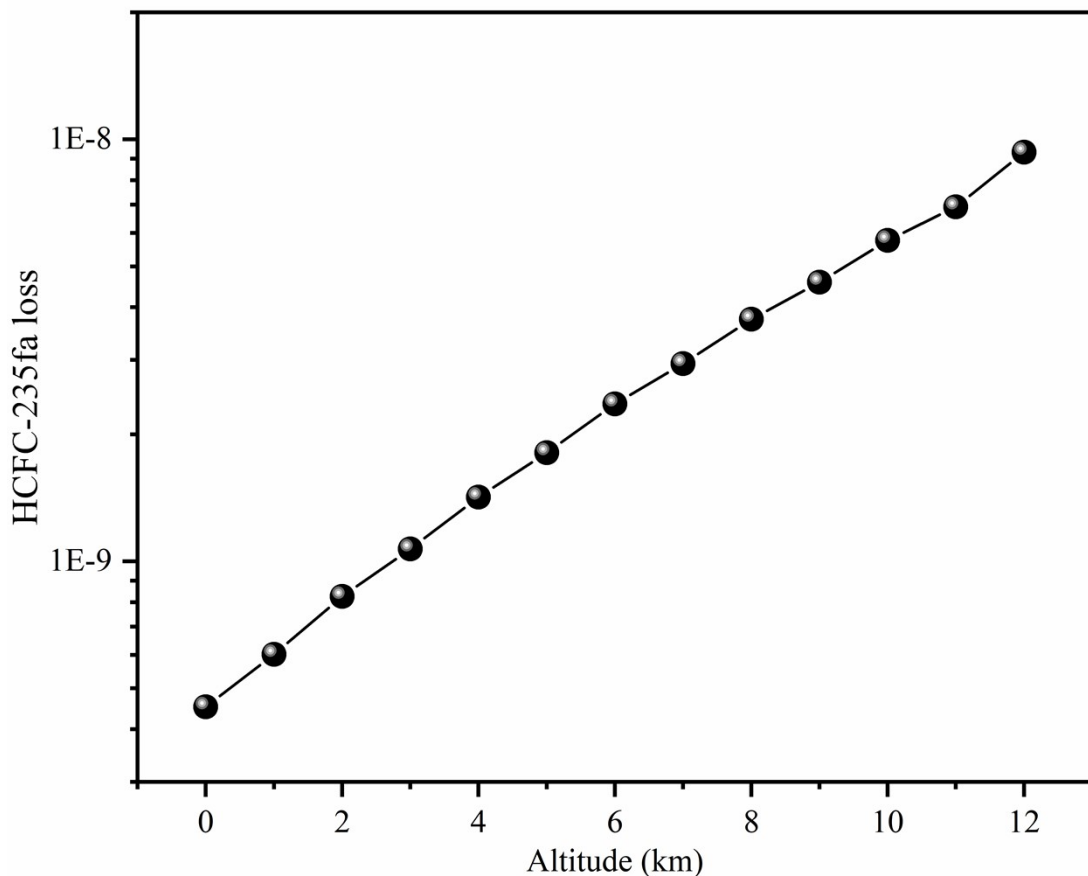


**Figure S3.** Calculated HCFC-235fa loss against altitude in the troposphere (different temperatures). ( $L^{HCFC-235fa} = k^{HCFC-235fa} \times [OH]$ ) (Where  $[OH]$  is the concentration of OH radical ( $[OH]=10^6$  molecule cm $^{-3}$ ) and  $k^{HCFC-235fa}$  denotes the rate constant of HCFC-235fa reacting with OH radical at 216.69-298.15 K.  $L^{HCFC-235fa}$  shows the ability that HCFC-235fa can react with OH radical to form  $CF_3C\cdot HCClF_2$  radical.) The rate coefficients were calculated at the CCSD(T)/aug-cc-pVTZ//M06-2X/6-311+G(d,p) level.

**Table S1a.** Calculated frequencies ( $\text{cm}^{-1}$ ) of the reactants, products, transition states and complexes at the level of M06-2X/6-311+G (d,p). (The value of the scaling factor is 0.970)

CF <sub>3</sub> CH <sub>2</sub> CClF <sub>2</sub> (R1a)	24.69, 102.62, 134.64, 232.64, 283.94, 304.36, 364.42, 415.88, 427.91, 515.43, 529.46, 584.22, 636.58, 817.09, 843.06, 905.42, 968.40, 1063.11, 1185.25, 1212.11, 1236.99, 1287.38, 1306.03, 1385.27, 1412.24, 3016.32, 3075.28
CF <sub>3</sub> CH <sub>2</sub> CClF <sub>2</sub> (R1b)	37.26, 101.70, 135.36, 241.04, 289.51, 316.25, 373.85, 399.28, 435.71, 515.78, 530.78, 593.55, 682.28, 694.06, 862.01, 898.75, 1005.94, 1097.68, 1162.24, 1205.26, 1220.87, 1282.15, 1299.94, 1396.06, 1417.49, 3010.34, 3075.70
P1	30.89, 59.74, 133.55, 237.57, 289.55, 307.53, 312.40, 391.51, 417.94, 491.15, 514.49, 586.94, 600.29, 689.23, 735.52, 878.12, 983.15, 1092.22, 1157.43, 1202.16, 1224.00, 1290.49, 1401.19, 3155.34
TS1a	-1610.16, 32.55, 57.64, 83.71, 124.28, 139.88, 199.38, 233.68, 293.95, 312.44, 322.65, 394.00, 431.75, 514.99, 527.28, 592.39, 669.17, 685.31, 731.65, 819.82, 867.74, 928.95, 982.24, 1098.99, 1106.56, 1198.76, 1219.26, 1227.54, 1271.73, 1371.08, 1393.97, 3062.84, 3662.78
TS2a	-906.16, 16.80, 39.19, 54.61, 108.19, 148.33, 214.04, 285.33, 309.33, 326.18, 391.24, 427.93, 443.72, 518.56, 532.10, 592.13, 665.81, 705.35, 749.16, 807.08, 874.39, 951.89, 1073.00, 1109.12, 1194.88, 1222.46, 1227.63, 1281.26, 1374.19, 3090.50
ER1a	34.64, 74.72, 85.85, 121.98, 144.52, 158.93, 244.41, 249.31, 292.95, 317.37, 365.60, 393.33, 405.10, 440.82, 518.58, 530.02, 593.48, 681.86, 697.68, 857.50, 897.63, 999.70, 1098.65, 1166.66, 1206.55, 1209.64, 1273.51, 1299.97, 1402.42, 1417.25, 3018.16, 3080.23, 3669.51
ER2a	19.63, 39.18, 48.76, 76.07, 120.02, 150.58, 245.90, 290.74, 316.65, 383.67, 404.15, 438.49, 514.54, 528.89, 591.92, 682.03, 698.03, 861.39, 896.90, 1001.41, 1098.76, 1164.66, 1205.43, 1209.23, 1279.92, 1297.61, 1398.07, 1419.87, 3020.00, 3080.55
EP1a	31.85, 59.92, 87.26, 103.61, 134.94, 138.62, 193.67, 241.32, 250.62, 259.22, 298.75, 317.44, 346.50, 391.87, 417.00, 482.14, 517.08, 581.59, 598.77, 689.12, 725.08, 879.58, 989.52, 1091.77, 1142.75, 1184.46, 1223.03, 1282.16, 1402.82, 1570.27, 3169.28, 3769.36, 3871.73
EP2a	21.23, 31.79, 52.84, 81.91, 85.41, 133.46, 168.03, 224.65, 287.37, 301.41, 312.49, 317.56, 397.55, 413.86, 474.29, 514.40, 576.14, 596.38, 680.20, 762.44, 869.46, 960.20, 1102.17, 1141.01, 1207.12, 1226.31, 1271.79, 1396.86, 2887.28, 3174.58
OH	3653.18
H <sub>2</sub> O	1547.36, 3779.00, 3881.83
HCl	2924.22

**Table S1b.** Relative Energies (in kcal/mol) of the reactions of  $\text{CF}_3\text{CH}_2\text{CClF}_2$  (R1a) + OH/Cl calculated at the CBS-QB3, CCSD(T)/6-311++G(d,p)//M06-2X/6-311+G(d,p) and CCSD(T)/aug-cc-pVTZ//M06-2X/6-311+G(d,p) levels of theory.

	CBS-QB3	CCSD(T)/6-311++G(d,p)	CCSD(T)/aug-cc-pVTZ
R1a+ OH	0.00	0.00	0.00
ER1	-2.29	-1.72	-1.52
TS1	3.81	6.42	4.89
EP1	-16.27	-14.34	-14.82
P1+H <sub>2</sub> O	-14.13	-10.75	-12.51
R1a+Cl	0.00	0.00	0.00
ER2	-2.01	-2.09	-1.11
TS2	5.48	9.64	7.75
EP2	-1.68	0.72	0.44
P1+HCl	0.37	4.47	2.46

**Table S1c.** Relative Energies (in kcal/mol) of the reactions of  $\text{CF}_3\text{CH}_2\text{CClF}_2$  (R1a) + OH/Cl calculated at M062-X/6-311+G(d,p) level of theory.

M06-2X/6-311+G(d,p)			
R1a+ OH	0.00	R1a+ Cl	0.00
ER13	-4.20	ER16	-1.58
TS13	32.24	TS16	68.89
EP13	30.26	EP16	67.62
P13+HClO	33.35	P15+FCl	70.06
R1a+OH	0.00	R1a+Cl	0.00
ER14	-4.23	ER17	-1.92
TS14	77.12	TS17	63.03
EP14	68.88	EP17	59.70
P14+HFO	72.73	P14+FCl	62.50
R1a+OH	0.00		
ER15	-4.15		
TS15	84.06		
EP15	76.60		
P15+HFO	80.29		

**Table S1d.** The change of Gibbs free energy and Enthalpies (in kcal/mol) of the reactions of  $\text{CF}_3\text{CH}_2\text{CClF}_2$  (R1a) + OH/Cl calculated at the CBS-QB3, CCSD(T)/6-311++G(d,p)//M06-2X/6-311+G(d,p) and CCSD(T)/aug-cc-pVTZ//M06-2X/6-311+G(d,p) levels of theory.

	CBS-QB3		CCSD(T)/6-311++G(d,p)		CCSD(T)/aug-cc-pVTZ	
	$\Delta G$	$\Delta H$	$\Delta G$	$\Delta H$	$\Delta G$	$\Delta H$
R1a + OH	-15.43	-13.62	-11.76	-10.31	-13.52	-12.06
R1a + Cl	-1.86	1.18	2.55	5.20	0.55	3.19

**Table S2a.** Multistructural torsional anharmonicity factors of  $\text{CF}_3\text{CH}_2\text{CClF}_2$ , TS1a and  $\text{CF}_3\text{CH}_2\text{CClF}_2 + \text{OH}$ , as well as the rate coefficients ( $\text{cm}^3 \text{molecule}^{-1} \text{s}^{-1}$ ) of TST, CVT, CVT/TST, SCT, CVT/SCT and MS-CVT/SCT for the reaction of  $\text{CF}_3\text{CH}_2\text{CClF}_2 + \text{OH}$  at 200–1000 K. <sup>a</sup>CCSD(T)/6-311++G(d,p)//M06-2X/6-311+G(d,p) level. <sup>b</sup>CCSD(T)/aug-cc-pVTZ//M06-2X/6-311+G(d,p) level.)

T (K)	F <sub>R</sub>	F <sub>TS</sub>	F <sub>act</sub>	TST	CVT <sup>a</sup>	CVT/TST <sup>a</sup>	SCT <sup>a</sup>	CVT/SCT <sup>a</sup>	MS-CVT/SCT <sup>a</sup>	MS-CVT/SCT <sup>b</sup>
200	1.534	1.959	1.277	2.46E-17	2.38E-17	0.967	2.164	5.15E-17	6.58E-17	1.88E-16
220	1.585	2.094	1.321	1.01E-16	9.80E-17	0.970	1.857	1.82E-16	2.40E-16	5.23E-16
240	1.631	2.225	1.364	3.31E-16	3.23E-16	0.976	1.666	5.38E-16	7.34E-16	1.27E-15
250	1.653	2.288	1.384	5.60E-16	5.48E-16	0.979	1.595	8.74E-16	1.21E-15	1.88E-15
253	1.660	2.307	1.390	6.52E-16	6.38E-16	0.979	1.567	1.00E-15	1.39E-15	2.11E-15
268	1.690	2.399	1.420	1.32E-15	1.30E-15	0.985	1.485	1.93E-15	2.74E-15	3.63E-15
272	1.698	2.423	1.427	1.58E-15	1.55E-15	0.981	1.471	2.28E-15	3.25E-15	4.15E-15
278	1.709	2.459	1.439	2.04E-15	2.00E-15	0.980	1.445	2.89E-15	4.16E-15	5.06E-15
283	1.718	2.488	1.448	2.50E-15	2.46E-15	0.984	1.427	3.51E-15	5.08E-15	5.94E-15
288	1.727	2.517	1.457	3.05E-15	3.00E-15	0.984	1.410	4.23E-15	6.16E-15	6.92E-15
297	1.743	2.569	1.474	4.30E-15	4.24E-15	0.986	1.377	5.84E-15	8.61E-15	9.05E-15
298	1.745	2.575	1.476	4.47E-15	4.40E-15	0.984	1.373	6.04E-15	8.91E-15	9.33E-15
301	1.750	2.592	1.481	4.98E-15	4.91E-15	0.986	1.365	6.70E-15	9.92E-15	1.02E-14
311	1.767	2.648	1.499	7.08E-15	6.98E-15	0.986	1.337	9.33E-15	1.40E-14	1.34E-14
318	1.778	2.687	1.511	8.95E-15	8.83E-15	0.987	1.314	1.16E-14	1.75E-14	1.62E-14
328	1.794	2.742	1.528	1.23E-14	1.22E-14	0.992	1.287	1.57E-14	2.40E-14	2.08E-14
331	1.798	2.758	1.534	1.35E-14	1.33E-14	0.985	1.293	1.72E-14	2.64E-14	2.24E-14
335	1.804	2.779	1.540	1.52E-14	1.50E-14	0.987	1.287	1.93E-14	2.97E-14	2.46E-14
345	1.818	2.832	1.558	2.04E-14	2.01E-14	0.985	1.264	2.54E-14	3.96E-14	3.10E-14

350	1.825	2.858	1.566	2.34E-14	2.32E-14	0.991	1.250	2.90E-14	4.54E-14	3.48E-14
363	1.843	2.924	1.587	3.32E-14	3.28E-14	0.988	1.235	4.05E-14	6.43E-14	4.60E-14
368	1.850	2.949	1.594	3.77E-14	3.73E-14	0.989	1.225	4.57E-14	7.28E-14	5.10E-14
372	1.855	2.969	1.601	4.17E-14	4.13E-14	0.990	1.218	5.03E-14	8.05E-14	5.52E-14
400	1.889	3.104	1.643	8.00E-14	7.93E-14	0.991	1.185	9.40E-14	1.54E-13	9.42E-14
455	1.946	3.350	1.721	2.34E-13	2.33E-13	0.996	1.137	2.65E-13	4.56E-13	2.29E-13
500	1.985	3.532	1.779	4.84E-13	4.81E-13	0.994	1.112	5.35E-13	9.52E-13	4.23E-13
550	2.023	3.716	1.837	9.61E-13	9.58E-13	0.997	1.086	1.04E-12	1.91E-12	7.62E-13
600	2.055	3.882	1.889	1.73E-12	1.73E-12	1.000	1.075	1.86E-12	3.51E-12	1.27E-12
650	2.082	4.032	1.937	2.90E-12	2.89E-12	0.997	1.062	3.07E-12	5.95E-12	1.99E-12
700	2.105	4.166	1.979	4.56E-12	4.56E-12	1.000	1.050	4.79E-12	9.48E-12	2.97E-12
750	2.125	4.286	2.017	6.84E-12	6.83E-12	0.999	1.042	7.12E-12	1.44E-11	4.26E-12
800	2.143	4.394	2.050	9.83E-12	9.82E-12	0.999	1.039	1.02E-11	2.09E-11	5.91E-12
850	2.158	4.489	2.080	1.37E-11	1.36E-11	0.993	1.037	1.41E-11	2.93E-11	7.95E-12
900	2.171	4.573	2.106	1.84E-11	1.84E-11	1.000	1.027	1.89E-11	3.98E-11	1.04E-11
950	2.182	4.647	2.130	2.43E-11	2.42E-11	0.996	1.025	2.48E-11	5.28E-11	1.34E-11
1000	2.191	4.712	2.151	3.12E-11	3.12E-11	1.000	1.022	3.19E-11	6.86E-11	1.69E-11

**Table S2b.** Multistuctural torsional anharmonicity factors of  $\text{CF}_3\text{CH}_2\text{CClF}_2$ , TS2a and  $\text{CF}_3\text{CH}_2\text{CClF}_2 + \text{Cl}$ , as well as the rate coefficients ( $\text{cm}^3 \text{molecule}^{-1} \text{s}^{-1}$ ) of TST, CVT, CVT/TST, SCT, CVT/SCT and MS-CVT/SCT for the reaction of  $\text{CF}_3\text{CH}_2\text{CClF}_2 + \text{Cl}$  at 200–1000 K. (<sup>a</sup>CCSD(T)/6-311++G(d,p)//M06-2X/6-311+G(d,p) level.  
<sup>b</sup>CCSD(T)/aug-cc-pVTZ//M06-2X/6-311+G(d,p) level.)

T	$F_R$	$F_{TS}$	$F_{act}$	TST <sup>a</sup>	CVT <sup>a</sup>	CVT/TST <sup>a</sup>	SCT <sup>a</sup>	CVT/SCT <sup>a</sup>	MS-CVT/SCT <sup>a</sup>	MS-CVT/SCT <sup>b</sup>
200	1.534	1.203	0.784	2.78E-20	2.39E-20	0.860	2.071	4.95E-20	3.88E-20	8.47E-20
220	1.585	1.228	0.775	1.87E-19	1.63E-19	0.872	1.809	2.94E-19	2.28E-19	3.73E-19
240	1.631	1.252	0.768	9.25E-19	8.13E-19	0.879	1.642	1.33E-18	1.02E-18	1.30E-18
250	1.653	1.263	0.764	1.88E-18	1.66E-18	0.883	1.576	2.61E-18	1.99E-18	2.28E-18
253	1.66	1.267	0.763	2.30E-18	2.03E-18	0.883	1.552	3.16E-18	2.41E-18	2.66E-18
268	1.69	1.284	0.760	5.94E-18	5.27E-18	0.887	1.478	7.79E-18	5.92E-18	5.61E-18
278	1.709	1.295	0.758	1.06E-17	9.41E-18	0.888	1.439	1.35E-17	1.02E-17	8.87E-18
283	1.718	1.301	0.757	1.39E-17	1.24E-17	0.892	1.411	1.76E-17	1.33E-17	1.10E-17
288	1.727	1.306	0.756	1.81E-17	1.62E-17	0.895	1.404	2.27E-17	1.72E-17	1.35E-17
297	1.743	1.316	0.755	2.86E-17	2.56E-17	0.895	1.373	3.51E-17	2.65E-17	1.95E-17
298	1.745	1.317	0.755	3.01E-17	2.69E-17	0.894	1.369	3.68E-17	2.78E-17	2.02E-17
301	1.75	1.32	0.754	3.48E-17	3.12E-17	0.897	1.357	4.24E-17	3.20E-17	2.27E-17
311	1.767	1.331	0.753	5.55E-17	4.98E-17	0.897	1.333	6.63E-17	4.99E-17	3.28E-17
318	1.778	1.338	0.753	7.56E-17	6.79E-17	0.898	1.316	8.94E-17	6.73E-17	4.19E-17
328	1.794	1.348	0.751	1.15E-16	1.04E-16	0.904	1.301	1.34E-16	1.01E-16	5.85E-17
331	1.798	1.352	0.752	1.30E-16	1.17E-16	0.900	1.282	1.51E-16	1.14E-16	6.46E-17
335	1.804	1.356	0.752	1.53E-16	1.37E-16	0.895	1.277	1.76E-16	1.32E-16	7.33E-17
345	1.818	1.366	0.751	2.24E-16	2.02E-16	0.902	1.264	2.55E-16	1.92E-16	9.92E-17
350	1.825	1.371	0.751	2.69E-16	2.43E-16	0.903	1.252	3.04E-16	2.28E-16	1.15E-16

363	1.843	1.383	0.750	4.24E-16	3.84E-16	0.906	1.233	4.73E-16	3.55E-16	1.65E-16
368	1.85	1.388	0.750	5.01E-16	4.54E-16	0.906	1.226	5.56E-16	4.17E-16	1.89E-16
372	1.855	1.392	0.750	5.71E-16	5.17E-16	0.905	1.219	6.31E-16	4.74E-16	2.10E-16
400	1.889	1.418	0.751	1.33E-15	1.21E-15	0.910	1.182	1.44E-15	1.08E-15	4.14E-16
455	1.946	1.467	0.754	5.31E-15	4.84E-15	0.911	1.139	5.52E-15	4.16E-15	1.27E-15
500	1.985	1.504	0.758	1.33E-14	1.22E-14	0.917	1.107	1.36E-14	1.03E-14	2.67E-15
550	2.023	1.542	0.762	3.16E-14	2.89E-14	0.915	1.094	3.15E-14	2.40E-14	5.43E-15
600	2.055	1.578	0.768	6.56E-14	6.00E-14	0.915	1.077	6.45E-14	4.95E-14	9.98E-15
650	2.082	1.612	0.774	1.23E-13	1.12E-13	0.911	1.063	1.20E-13	9.29E-14	1.69E-14
700	2.105	1.644	0.781	2.13E-13	1.94E-13	0.911	1.052	2.05E-13	1.60E-13	2.68E-14
750	2.125	1.673	0.787	3.44E-13	3.15E-13	0.916	1.045	3.29E-13	2.59E-13	4.04E-14
800	2.143	1.701	0.794	5.28E-13	4.83E-13	0.915	1.040	5.01E-13	3.98E-13	5.83E-14
850	2.158	1.726	0.800	7.75E-13	7.07E-13	0.912	1.033	7.30E-13	5.84E-13	8.16E-14
900	2.171	1.75	0.806	1.10E-12	9.99E-13	0.908	1.023	1.03E-12	8.30E-13	1.10E-13
950	2.182	1.772	0.812	1.50E-12	1.37E-12	0.913	1.022	1.40E-12	1.14E-12	1.45E-13
1000	2.191	1.791	0.817	2.00E-12	1.82E-12	0.910	1.022	1.85E-12	1.51E-12	1.86E-13

**Table S3a.** Zero-point energy (ZPE), vibrational ground-state adiabatic potential energy ( $V_a^G$ ) and classical potential energy ( $V_{MEP}$ ) for the reaction of  $\text{CF}_3\text{CH}_2\text{CClF}_2 + \text{OH}$  as functions of the intrinsic coordinate  $s$  (amu) $^{1/2}$ bohr at the M06-2X/6-311+G(d,p) level.

$s$ (bohr)	$V_{MEP}$	$V_a^G$	ZPE
-1.46	2.34	44.07	41.73
-1.38	2.58	44.26	41.68
-1.30	2.82	44.46	41.64
-1.22	3.09	44.66	41.57
-1.13	3.37	44.89	41.52
-1.05	3.66	45.13	41.47
-0.97	3.97	45.39	41.42
-0.89	4.30	45.65	41.35
-0.81	4.64	45.93	41.29
-0.73	4.99	46.21	41.22
-0.65	5.29	46.45	41.16
-0.57	5.53	46.62	41.09
-0.49	5.71	46.75	41.04
-0.41	5.84	46.83	40.99
-0.32	5.92	46.86	40.94
-0.24	5.95	46.85	40.90
-0.16	5.94	46.80	40.86
-0.08	5.88	46.71	40.83
0.00	5.79	46.60	40.81
0.08	5.66	46.45	40.79
0.16	5.50	46.27	40.77
0.24	5.30	46.05	40.75
0.32	5.04	45.79	40.75
0.41	4.72	45.48	40.76
0.49	4.34	45.10	40.76
0.57	3.88	44.65	40.77
0.65	3.35	44.14	40.79
0.73	2.76	43.57	40.81
0.81	2.09	42.92	40.83
0.89	1.35	42.22	40.87
0.97	0.55	41.45	40.90
1.05	-0.32	40.63	40.95
1.13	-1.25	39.74	40.99
1.22	-2.25	38.79	41.04
1.30	-3.31	37.79	41.10
1.38	-4.43	36.73	41.16
1.46	-5.62	35.61	41.23

**Table S3b.** Zero-point energy (ZPE), vibrational ground-state adiabatic potential energy ( $V_a^G$ ) and classical potential energy ( $V_{MEP}$ ) for the reaction of  $\text{CF}_3\text{CH}_2\text{CClF}_2 + \text{Cl}$  as functions of the intrinsic coordinate  $s$  (amu) $^{1/2}$ bohr at the M06-2X/6-311+G(d,p) level.

$s$ (bohr)	$V_{MEP}$	$V_a^G$	ZPE
-1.44	6.56	41.05	34.49
-1.35	6.81	41.21	34.4
-1.26	7.07	41.38	34.31
-1.17	7.34	41.58	34.24
-1.08	7.61	41.79	34.18
-0.99	7.89	42.02	34.13
-0.9	8.18	42.26	34.08
-0.81	8.47	42.48	34.01
-0.72	8.75	42.68	33.93
-0.63	9.02	42.87	33.85
-0.54	9.26	43.04	33.78
-0.45	9.48	43.19	33.71
-0.36	9.67	43.31	33.64
-0.27	9.84	43.40	33.56
-0.18	9.97	43.45	33.48
-0.09	10.05	43.46	33.41
0.00	10.08	43.42	33.34
0.09	10.07	43.33	33.26
0.18	10.03	43.23	33.2
0.27	9.98	43.10	33.12
0.36	9.90	42.95	33.05
0.45	9.80	42.78	32.98
0.54	9.68	42.58	32.9
0.63	9.53	42.37	32.84
0.72	9.36	42.12	32.76
0.81	9.16	41.86	32.7
0.90	8.95	41.57	32.62
0.99	8.70	41.26	32.56
1.08	8.44	40.93	32.49
1.17	8.16	40.57	32.41
1.26	7.85	40.19	32.34
1.35	7.51	39.79	32.28
1.44	7.16	39.37	32.21

**Table S4a.** Calculated atmospheric lifetime ( $\tau$ ) values for  $\text{CF}_3\text{CH}_2\text{CClF}_2$  determined by OH radical at variable temperatures (T) and altitudes (H) in the earth atmosphere according to the rate coefficients ( $k_{\text{OH}}^{\text{MS} - \text{CVT/SCT}}$ ). The rate coefficients were calculated at the CCSD(T)/aug-cc-pVTZ//M06-2X/6-311+G(d,p) level.

T(K)	<sup>a</sup> [OH]	$k^{\text{MS} - \text{H}}$ (km)	$k_{\text{OH}}^{\text{MS} - \text{CVT/SCT}}$								
			9.0E+05	9.7E+05	1.0E+06	1.5E+06	2.0E+06	3.0E+06	5.0E+06	1.0E+07	1.5E+07
216.69	4.52E-16	12	77.93	72.30	70.13	46.76	35.07	23.38	14.03	7.01	4.68
223.29	6.02E-16	10	58.57	54.35	52.71	35.14	26.36	17.57	10.54	5.27	3.51
229.78	8.26E-16	9	42.68	39.60	38.41	25.61	19.20	12.80	7.68	3.84	2.56
236.27	1.07E-15	8	32.90	30.52	29.61	19.74	14.80	9.87	5.92	2.96	1.97
242.76	1.42E-15	7	24.73	22.94	22.26	14.84	11.13	7.42	4.45	2.23	1.48
249.25	1.81E-15	6	19.46	18.05	17.51	11.68	8.76	5.84	3.50	1.75	1.17
255.74	2.36E-15	5	14.94	13.86	13.44	8.96	6.72	4.48	2.69	1.34	0.90
262.23	2.94E-15	4	11.98	11.11	10.78	7.19	5.39	3.59	2.16	1.08	0.72
268.72	3.75E-15	3	9.39	8.71	8.45	5.63	4.23	2.82	1.69	0.85	0.56
275.21	4.59E-15	2	7.68	7.13	6.91	4.61	3.46	2.30	1.38	0.69	0.46
281.70	5.76E-15	1	6.12	5.68	5.51	3.67	2.75	1.84	1.10	0.55	0.37
288.19	6.92E-15	0	5.09	4.72	4.58	3.05	2.29	1.53	0.92	0.46	0.31
298.15	9.33E-15	0	3.78	3.51	3.40	2.27	1.70	1.13	0.68	0.34	0.23

<sup>a</sup>Herein, the [OH] is from references [6-8] (unit:molecule cm<sup>-3</sup>); <sup>b</sup>Unit: year

**Table S4b.** Calculated atmospheric lifetime ( $\tau$ ) values for  $\text{CF}_3\text{CH}_2\text{CClF}_2$  determined by Cl atom at different temperatures (T) and altitudes (H) in the earth atmosphere according to the rate coefficients ( $k_{\text{Cl}}^{\text{MS} - \text{CVT/SCT}}$ ). The rate coefficients were calculated at the CCSD(T)/aug-cc-pVTZ//M06-2X/6-311+G(d,p) level.

T(K)	<sup>a</sup> [Cl]	$k^{\text{MS} - \text{CVT/SCT}}$	H (km)	$k^{\text{MS} - \text{CVT/SCT}}$								
				1.0E+03	2.0E+03	5.0E+03	1.0E+04	2.0E+04	5.0E+04	1.0E+05	5.0E+05	1.0E+06
216.69	3.03E-19		12	1045.54	522.77	209.11	104.55	52.28	20.91	10.46	2.09	1.05
223.29	4.55E-19		10	696.25	348.12	139.25	69.62	34.81	13.92	6.96	1.39	0.70
229.78	7.15E-19		9	443.38	221.69	88.68	44.34	22.17	8.87	4.43	0.89	0.44
236.27	1.03E-18		8	307.80	153.90	61.56	30.78	15.39	6.16	3.08	0.62	0.31
242.76	1.55E-18		7	204.89	102.44	40.98	20.49	10.24	4.10	2.05	0.41	0.20
249.25	2.16E-18		6	147.11	73.55	29.42	14.71	7.36	2.94	1.47	0.29	0.15
255.74	3.12E-18		5	101.70	50.85	20.34	10.17	5.09	2.03	1.02	0.20	0.10
262.23	4.21E-18		4	75.35	37.67	15.07	7.53	3.77	1.51	0.75	0.15	0.08
268.72	5.89E-18		3	53.88	26.94	10.78	5.39	2.69	1.08	0.54	0.11	0.05
275.21	7.74E-18		2	40.98	20.49	8.20	4.10	2.05	0.82	0.41	0.08	0.04
281.70	1.05E-17		1	30.14	15.07	6.03	3.01	1.51	0.60	0.30	0.06	0.03
288.19	1.35E-17		0	23.43	11.71	4.69	2.34	1.17	0.47	0.23	0.05	0.02
298.15	2.02E-17		0	15.68	7.84	3.14	1.57	0.78	0.31	0.16	0.03	0.02

<sup>a</sup>Herein, the [Cl] is from references <sup>[9-10]</sup> (unit:molecule cm<sup>-3</sup>); <sup>b</sup>Unit: hundred thousand years

**Table S4c.** Calculated OH-controlled, Cl-controlled and effective atmospheric lifetime (unit: years) of CF<sub>3</sub>CH<sub>2</sub>CClF<sub>2</sub> at minimum [OH] of 9.0×10<sup>5</sup> molecules cm<sup>-3</sup> and at maximum [Cl] of 10<sup>6</sup> atoms cm<sup>-3</sup> at variable temperatures (T) and altitudes (H).

T(K)	H (km)	OH-controlled (years)	Cl-controlled (years)	effective lifetime (years)
216.69	12	77.93	104554.38	77.87
223.29	11	58.57	69624.66	58.52
229.78	10	42.68	44338.38	42.63
236.27	9	32.90	30780.31	32.86
242.76	8	24.73	20488.60	24.70
249.25	7	19.46	14710.65	19.43
255.74	6	14.94	10170.48	14.92
262.23	5	11.98	7534.76	11.96
268.72	4	9.39	5387.52	9.37
275.21	3	7.68	4097.75	7.67
281.70	2	6.12	3013.61	6.11
288.19	1	5.09	2342.55	5.08
298.15	0	3.78	1567.72	3.77

**Table S5.** Calculated atmospheric lifetimes at 216.69-298.15 K and global warming potentials (GWP<sub>s</sub>) of CF<sub>3</sub>CH<sub>2</sub>CClF<sub>2</sub> for the time horizons of 20, 100, and 500 years at the level of CCSD(T)/aug-cc-pVTZ//M06-2X/6-311+G(d,p).

Atmospheric lifetime (years)	GWP <sub>s</sub>		
	20 years	100 years	500 years
0.23	74.14	21.06	6.40
60	5482.45	4455.65	1670.04
77.93	5686.05	5157.35	2166.08

**Table S6.** ECOSAR toxicity values of  $\text{CF}_3\text{CH}_2\text{CClF}_2$  (R1a) and its degradation products to aquatic organisms (unit:  $\text{mg L}^{-1}$ ).

	Organism	R1a	IM3	IM6	IM11	IM12
Acute toxicity	Fish LC <sub>50</sub>	19.04	1428.92	35.33	36.99	46.21
	Daphnid LC <sub>50</sub>	11.81	733.65	21.62	122.20	178.47
	Green Algae EC <sub>50</sub>	12.69	360.43	21.94	134.69	183.24
Chronic toxicity	Fish ChV	2.07	99.68	3.77	5.04	5.99
	Daphnid ChV	1.47	54.06	2.60	13.59	18.71
	Green Algae ChV	4.05	75.43	6.79	35.52	45.12

**Table S7.** The acute and chronic toxic class (unit: mg L<sup>-1</sup>).

Classification	Acute toxicity <sup>a</sup>	Chronic toxicity <sup>b</sup>
Not harmful	LC <sub>50</sub> >100 or EC <sub>50</sub> >100	ChV>10
Harmful	10<LC <sub>50</sub> <100 or 10<EC <sub>50</sub> <100	1<ChV<10
Toxic	1<LC <sub>50</sub> <10 or 1<EC <sub>50</sub> <10	0.1<ChV<1
Very toxic	LC <sub>50</sub> <1 or EC <sub>50</sub> <1	ChV<0.1

<sup>a</sup> Criteria set by the European Union (described in Annex VI of Directive 67/548/EEC);

<sup>b</sup> Criteria set by the Chinese hazard evaluation guidelines for new chemical substances (HJ/T154–2004).

## References

- (1) J. B. Burkholder, R. A. Cox and A. R. Ravishankara, *Chem. Rev.*, 2015, **115**, 3704-3759.
- (2) F. Y. Bai, S. Lv, Y. Ma, C. Y. Liu, C. F. He and X. M. Pan, *Chemosphere*, 2017, **171**, 49-56.
- (3) G. Manonmani, L. Sandhiya and K. Senthilkumar, *J. Phys. Chem. A*, 2022, **126**, 9564-9576.
- (4) G. Manonmani, L. Sandhiya and K. Senthilkumar, *Environ. Sci. Pollut. Res.*, 2023, **30**, 50209-50224.
- (5) F. A. de Leeuw, *Chemosphere*, 1993, **27**, 1313-1328
- (6) M. G. Lawrence, P. Jöckel and R. Von Kuhlmann, *Atmos. Chem. Phys.*, 2001, **1**, 37-49.
- (7) D. Chakraborty and G. Lehmann, *J. Solid. State. Chem.*, 1976, **17**, 305-311.
- (8) D. E. Heard and M. J. Pilling, *Chem. Rev.*, 2003, **103**, 5163-5198.
- (9) H. D. Osthoff, J. M. Roberts, A. R. Ravishankara, E. J. Williams, B. M. Lerner, R. Sommariva, T. S. Bates, D. Coffman, P. K. Quinn, J. E. Dibb, H. Stark, J. B. Burkholder, R. K. Talukdar, J. Meagher, F. C. Fehsenfeld and S. S. Brown, *Nature Geosci.*, 2008, **1**, 324-328.
- (10) O. W. Wingenter, D. R. Blake, N. J. Blake, B. C. Sive, F. S. Rowland, E. Atlas and F. Flocke, *J. Geophys. Res. Atmos.*, 1999, **104**, 21819-21828.